Polarization and Differential Cross Section for Neutrons Scattered from Li^6 and Li^7†

R. O. LANE, A. J. ELWYN, AND A. LANGSDORF, JR.
Argonne National Laboratory, Argonne, Illinois
(Received 13 August 1964)

The polarization and differential cross section for neutrons scattered from Li^6 and Li^7 have been measured at several angles for neutron energies from 0.2 to 2.0 MeV. The measurements indicate that for energies from about 0.5 to 2.0 MeV both Li^6 and Li^7 are useful as polarization analyzers. Attempts to explain both the differential cross section and polarization results simultaneously, for the n-Li^7 scattering in terms of only a few levels in the compound nucleus Li^8, are only partially successful. Furthermore, preliminary calculations based on an optical-model interaction for both the n-Li^6 and n-Li^7 scatterings do not lead to a completely successful interpretation of all the results.

INTRODUCTION

IN the study of the scattering of neutrons from the nuclei Li^6 and Li^7, energy levels in the compound nuclei Li^7 and Li^8, respectively, may be observed. The level structure of the nucleus Li^7 in the energy region above the neutron binding energy shows a state at 7.47 MeV, while the structure of Li^8 (also in the energy region above the neutron binding energy) shows levels at 2.26 and 3.22 MeV. No other higher energy states are known in either isotope.

Previous studies[1–3] of the differential cross section $\sigma(\theta)$ for neutrons elastically scattered from both Li^6 and Li^7 have confined themselves mainly to the region of the 7.47- and 2.26-MeV states, respectively, where resonances are observed in the total cross section for both nuclei at a neutron energy of about 0.25 MeV. The measurements have been consistent with spin and parity assignments of $J^\pi=\frac{5}{2}^-$ and $J^\pi=3^+$ for the states in Li^7 and Li^8, respectively, both states being formed by p-wave neutrons. One series[3] of measurements of the differential cross section extended above the resonances to a neutron energy of 2.2 MeV, where the cross sections become nearly independent of energy. Measurements[4] of γ rays from the reaction $Li^7(n,n')Li^{7*}$ to the 0.478-MeV level in Li^7 showed a broad level in Li^8 at an excitation energy of 3.22 MeV. The spin $J=1$ was assigned to this level, and positive parity was favored. A few later measurements of the scattering of neutrons from these nuclei have been performed at energies from 1.5 to 7.5 MeV,[5] and more recently at 14 MeV.[6] These higher-energy results have been interpreted in terms of an optical-model interaction between the neutrons and the nuclei in question.

Willard *et al.*[7] and Darden *et al.*[8] have measured the polarization $P(\theta)$ in the vicinity of the resonances in these nuclei. More recently, Elwyn and Lane[9] measured the polarization for neutrons scattered from Li^6 and Li^7 at 45° and 90° from the region of the resonances up to 2.4 MeV, where the values of polarization become nearly independent of energy. In the work reported here, we have made a more extensive systematic study of both the polarization and differential cross sections, especially in the energy range between 0.5 and 2.0 MeV. It was of interest to observe whether the results could be understood in terms of the few known energy states in the compound nuclei Li^7 and Li^8 and some postulated broad-scattering states, or if a more consistent explanation was to be found in an optical-model description, even at energies between 1 and 2 MeV. In connection with the present measurements, it should be mentioned that both Li^6 and Li^7 may be quite useful as analyzers in studies of the polarization of neutrons emitted in nuclear reactions.

EXPERIMENT

In earlier papers,[10] the apparatus and the analysis connected with the experimental arrangement have been discussed extensively. The reaction $Li^7(p,n)Be^7$ provided a partially polarized beam of neutrons emitted at 51° relative to the incident protons. A transverse magnetic field precessed the spins of the neutrons through 180° to provide the means of observing the product of the polarizations produced by the source and by the scattering. The partially polarized beam of neutrons was incident upon metallic scatterers of Li^6 (Li enriched to 96% Li^6) and Li^7 (natural abundance of 92.6%Li^7). The scatterers were slabs encased in steel cans with walls 0.005 in. thick. The large faces measured 10 in.×20 in., and the thicknesses were $\frac{1}{8}$ in., $\frac{1}{4}$ in., and $\frac{1}{2}$ in. for the Li^7 and $\frac{5}{32}$ in. and $\frac{5}{16}$ in. for the Li^6.

† Work performed under the auspices of the U. S. Atomic Energy Commission.

[1] R. G. Thomas, M. Walt, R. B. Walton, and R. C. Allen, Phys. Rev. **101**, 759 (1956).
[2] H. B. Willard, J. K. Bair, J. D. Kington, and H. O. Cohn, Phys. Rev. **101**, 765 (1956).
[3] R. O. Lane, A. Langsdorf, Jr., J. E. Monahan, and A. J. Elwyn, Ann. Phys. **12**, 135 (1961).
[4] J. M. Freeman, A. M. Lane, and B. Rose, Phil. Mag. **46**, 17 (1955).
[5] R. Batchelor and J. H. Towle, Nucl. Phys. **47**, 385 (1963); Phys. Letters **2**, 312 (1962).
[6] A. H. Armstrong, J. Gammel, L. Rosen, and G. M. Frye, Jr., Nucl. Phys. **52**, 505 (1964).
[7] H. B. Willard, J. K. Bair, H. O. Cohn, and J. D. Kington, Bull. Am. Phys. Soc. **1**, 54 (1956).
[8] S. E. Darden, T. R. Donoghue, and C. A. Kelsey, Nucl. Phys. **22**, 434 (1961).
[9] A. J. Elwyn and R. O. Lane, Nucl. Phys. **31**, 78 (1962).
[10] For a list of earlier papers and a description of the formalism employed for interpretation in terms of levels, see R. O. Lane, A. J. Elwyn, and A. Langsdorf, Jr., Phys. Rev. **133**, B409 (1964).

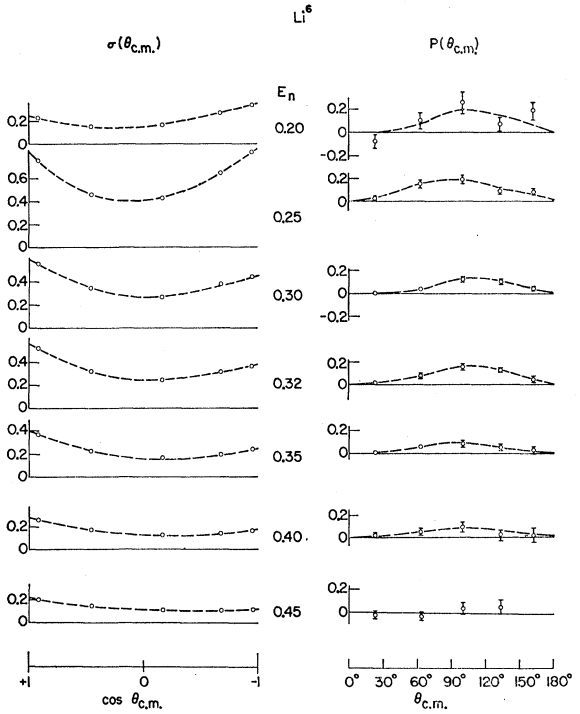

FIG. 1. Angular distributions of $\sigma(\theta)$ and $P(\theta)$ for Li^6 at incident energies of 0.20 through 0.45 MeV. The dashed curves are simply drawn through the points. Statistical errors on $\sigma(\theta)$ are less than 2%, while the total error is probably less than 5%. $\sigma(\theta)$ in this and following graphs is in barns per steradian.

The differential cross sections were corrected for multiple scattering by means of a Monte Carlo program.[10] The polarization data were corrected approximately, as described previously.[9,10] At all energies above 0.5 MeV, the transmission of the scattering samples was greater than 90%, so that the multiple-scattering effects were minimized. Corrections for the second group of neutrons from the source reaction were made on the assumption that this group is unpolarized. The data were also corrected for the effects of the minor isotopes in each sample, as well as for the energy dependence of the efficiency of each detector. The energy spread of the beam (produced mainly by the thickness of the Li target) was restricted to 10 keV on the resonances and 40 keV elsewhere, so that no correction was necessary for the effects of resolution. Above 0.54 MeV, inelastic scattering to the first excited state in Li^7 begins to take place. Our detectors do not discriminate against inelastically scattered neutrons; the differential cross sections presented here are, therefore, total (elastic plus inelastic) scattering cross sections. If we subtract the values of the elastic differential cross sections given by Batchelor and Towle[5] for n-Li^7 scattering at 1.5 MeV from our measurements at that energy, the resulting angular distribution is approximately isotropic and yields a total inelastic cross section amounting to only 10% of the measured total scattering cross sections. In the energy region in which inelastic scattering can occur, the total inelastic cross section reaches a maximum of about 12% of the total cross section. If the inelastic angular distributions are assumed to be isotropic and the inelastically scattered neutrons are assumed to be unpolarized, the values of $\sigma(\theta)$ and $P(\theta)$ (corrected to give the elastic results) are at most 10 to 12% larger than the results shown here. Since there is very little information concerning the polarization of inelastically scattered neutrons, and because we do not feel that the major conclusions in the present work would be affected by a correction of this size, no corrections were made for these effects.

RESULTS

Figures 1–6 show the experimental angular distributions of both $\sigma(\theta)$ and $P(\theta)$ for Li^6 and Li^7 at energies from 0.2 through 2.0 MeV. The Basel convention for the sign of $P(\theta)$ is used throughout. Values of the polarization for the $Li^7(p,n)Be^7$ reaction taken from Ref. 9 were used to derive the polarization $P(\theta)$ for scattering from Li^6 and Li^7 from the measured product of $P(\theta)$ and the source polarization. Since the polarization for

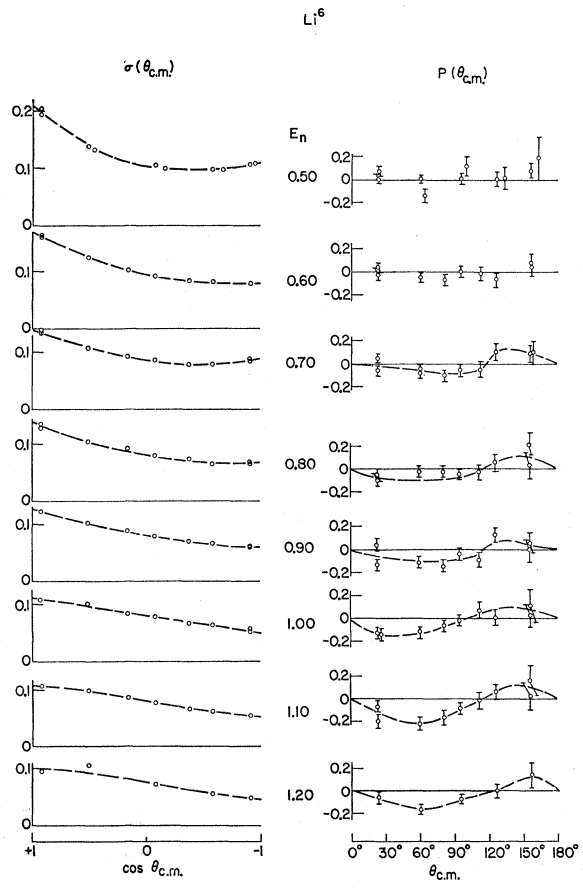

FIG. 2. Angular distributions of $\sigma(\theta)$ and $P(\theta)$ for Li^6 at incident energies of 0.5 through 1.2 MeV. The dashed curves are simply drawn through the points. Statistical errors on $\sigma(\theta)$ are less than 2%, while the total error is probably less than 5%.

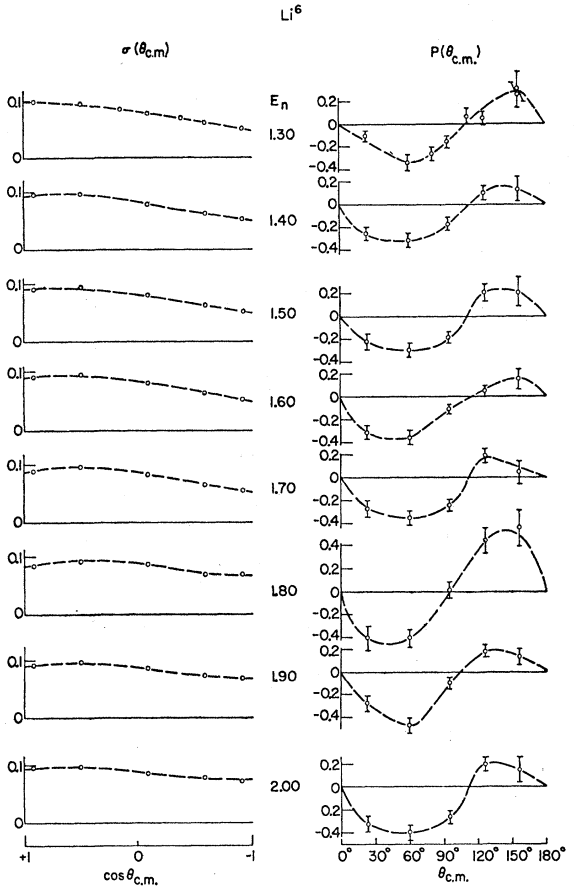

FIG. 3. Angular distributions of $\sigma(\theta)$ and $P(\theta)$ for Li^6 at incident energies of 1.3 through 2.0 MeV. The dashed curves are simply drawn through the points. Statistical errors on $\sigma(\theta)$ are less than 2%, while the total error is probably less than 5%.

these nuclides is large enough to make them useful as polarization analyzers, numerical values for $P(\theta)$ are given in Tables I–IV. Although these quantities usually were measured at only five angles, in some cases additional angles were included. The data for $\sigma(\theta)$ agree well with our earlier work[3] at eight angles.

On the resonance near 0.25 MeV, neutrons scattered by Li^7 are polarized as much as -60%, while neutrons scattered by Li^6 are polarized less than $+20\%$. As the energy increases, both the polarizations and differential

TABLE I. Polarization $P(\theta_{c.m.})$ for Li^6.

E_{lab} (MeV)	$P(\theta_{c.m.})$ 23°	63°	100°	133°	162°
0.20	−0.07 ±0.06	0.10 ±0.07	0.26 ±0.10	0.07 ±0.06	0.19 ±0.08
0.25	0.03 ±0.02	0.15 ±0.03	0.18 ±0.03	0.08 ±0.03	0.08 ±0.03
0.25	0.03 ±0.02	0.15 ±0.03	0.18 ±0.03	0.09 ±0.03	0.07 ±0.03
0.25	0.03 ±0.02	0.15 ±0.03	0.18 ±0.03	0.08 ±0.02	0.08 ±0.02
0.30	−0.00 ±0.01	0.03 ±0.01	0.12 ±0.02	0.09 ±0.02	0.03 ±0.02
0.32	0.02 ±0.01	0.07 ±0.02	0.15 ±0.03	0.12 ±0.02	0.04 ±0.03
0.35	0.00 ±0.01	0.05 ±0.02	0.08 ±0.03	0.05 ±0.03	0.03 ±0.03
0.40	0.03 ±0.02	0.05 ±0.03	0.09 ±0.04	0.02 ±0.04	0.01 ±0.06
0.45	−0.02 ±0.03	−0.03 ±0.04	0.04 ±0.05	0.06 ±0.06	0.24 ±0.10
0.50	0.07 ±0.05	−0.14 ±0.06	0.12 ±0.09	0.02 ±0.10	0.19 ±0.19

cross sections of the two nuclides seem to become more similar. This is especially true for the polarization, which tends mainly toward an angular dependence of the form $-A\sin 2\theta$ for both nuclides. Probably the most striking feature of these polarization results is the strong similarity between the data for the two nuclides at energies above 1 MeV. It is interesting to note that in measurements of the polarization of 14-MeV protons scattered from Li^6 and Li^7, Rosen and Leland[11] obtain results at angles less than 100° which are nearly the same as those reported here for a neutron energy of about 2 MeV. No polarization data for neutrons have been reported above 2.4 MeV. Such results are clearly needed to establish the true trend from low to high energies and would be a valuable adjunct to the corresponding proton data at 14 MeV.

Figures 7–10 show the energy variation of the coefficients B_L and C_L for Li^6 and Li^7 when the following expansions are made:

$$\sigma(\theta)=\sum_{L=0}^{2} B_L P_L(\cos\theta),$$

$$\sigma_p(\theta)\equiv\sigma(\theta)P(\theta)=\sum_{L=1}^{2} C_L P_L{}^1(\cos\theta),$$

where $P_L(\cos\theta)$ and $P_L{}^1(\cos\theta)$ are the ordinary and associated Lengendre polynomials of the first kind, respectively. For both nuclides, only terms through $L=2$ were necessary in the expansions. Within experimental errors, the higher terms were zero.

In the vicinity of the resonances near 0.25 MeV, both

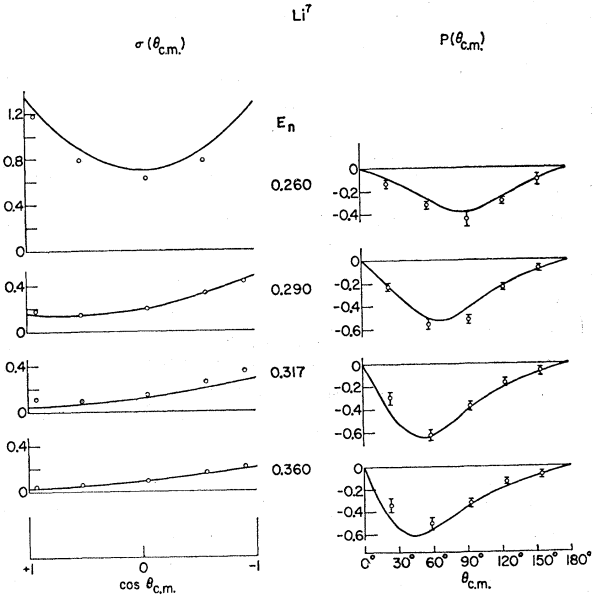

FIG. 4. Angular distributions of $\sigma(\theta)$ and $P(\theta)$ for Li^7 at incident energies of 0.26 through 0.36 MeV. The solid curves are the results of calculation (C) described in Table V. Statistical errors on $\sigma(\theta)$ are less than 2%, while the total error is probably less than 5%.

TABLE II. Polarization P ($\theta_{c.m.}$) for Li^6.

E_{lab} (MeV)	P ($\theta_{c.m.}$) 23°	60°	81°	95°	112°	126°	156°
0.5	0.00±0.03	−0.00±0.04		0.01±0.05		0.01±0.06	0.09±0.07
0.6	0.04±0.04			0.01±0.05		−0.06±0.06	0.08±0.08
0.6	−0.03±0.04	−0.05±0.04	−0.07±0.05		−0.01±0.06		0.05±0.09
0.7	0.04±0.04	−0.09±0.04		−0.06±0.05		0.10±0.07	0.09±0.08
0.7	−0.07±0.04	−0.05±0.04	−0.11±0.05		−0.05±0.07		0.10±0.10
0.8	−0.11±0.04			−0.05±0.05		0.05±0.07	0.21±0.11
0.8	−0.05±0.05	−0.03±0.05	−0.03±0.05		−0.03±0.07		0.03±0.12
0.9	−0.13±0.05			−0.04±0.05		0.12±0.07	0.05±0.09
0.9	0.04±0.05	−0.11±0.05	−0.14±0.06		−0.09±0.07		−0.01±0.11
1.0	−0.13±0.05			−0.02±0.05		0.01±0.07	0.02±0.10
1.0	−0.14±0.06	−0.13±0.05	−0.07±0.05		−0.07±0.07		0.10±0.14
1.1	−0.07±0.05			−0.09±0.05		0.05±0.06	0.01±0.10
1.1	−0.20±0.07	−0.22±0.05	−0.17±0.06		−0.02±0.07		0.15±0.13
1.2	−0.06±0.05	−0.16±0.04		−0.07±0.04		−0.00±0.06	0.14±0.11
1.3	−0.10±0.05			−0.16±0.05		0.05±0.06	0.25±0.11
1.3	−0.10±0.07	−0.33±0.07	−0.26±0.06		0.07±0.07		0.30±0.16
1.4	−0.25±0.06	−0.31±0.06		−0.17±0.05		0.10±0.06	0.13±0.11
1.5	−0.22±0.07	−0.29±0.06		−0.19±0.05		0.21±0.07	0.21±0.13
1.6	−0.31±0.06	−0.35±0.06		−0.11±0.04		0.05±0.05	0.15±0.09
1.7	−0.27±0.07	−0.35±0.06		−0.24±0.05		0.19±0.06	0.04±0.10
1.8	−0.40±0.11	−0.40±0.08		0.02±0.07		0.45±0.11	0.57±0.17
1.9	−0.27±0.07	−0.46±0.07		−0.09±0.05		0.19±0.05	0.14±0.07
2.0	−0.32±0.07	−0.40±0.06		−0.26±0.06		0.19±0.06	0.14±0.11

TABLE III. Polarization P ($\theta_{c.m.}$) for Li^7.

E_{lab} (MeV)	P ($\theta_{c.m.}$) 23°	58°	80°	93°	111°	124°	155°
0.26	−0.11±0.02	−0.32±0.03		−0.47±0.04		−0.29±0.03	−0.13±0.02
0.26	−0.13±0.02	−0.33±0.02		−0.44±0.04		−0.29±0.03	−0.10±0.02
0.29	−0.22±0.03	−0.55±0.04		−0.52±0.04		−0.23±0.02	−0.08±0.02
0.317	−0.35±0.04	−0.66±0.05		−0.39±0.03		−0.18±0.02	−0.04±0.02
0.317	−0.24±0.04	−0.58±0.05		−0.37±0.03		−0.18±0.03	−0.10±0.02
0.36	−0.34±0.06	−0.50±0.04		−0.33±0.03		−0.15±0.02	−0.08±0.02
0.50	−0.28±0.11	−0.50±0.09		−0.31±0.06		−0.17±0.04	−0.07±0.04
0.60	−0.10±0.08			−0.30±0.07		−0.15±0.05	−0.02±0.06
0.60	−0.16±0.09	−0.39±0.09	−0.22±0.06		−0.14±0.05		−0.00±0.08
0.70	−0.20±0.07	−0.28±0.07		−0.23±0.06		−0.06±0.04	−0.03±0.04
0.70	−0.27±0.08	−0.28±0.07	−0.21±0.06		−0.07±0.04		−0.03±0.03
0.80	−0.14±0.04	−0.24±0.05		−0.22±0.05		−0.07±0.06	−0.03±0.04
0.80	−0.22±0.07	−0.34±0.07	−0.22±0.06		−0.02±0.04		0.03±0.05
0.90	−0.25±0.06	−0.37±0.07		−0.16±0.04		0.05±0.03	0.01±0.04
1.00	−0.21±0.05	−0.30±0.05		−0.08±0.03		0.13±0.04	0.08±0.04
1.00	−0.13±0.05	−0.26±0.05	−0.20±0.04		−0.04±0.03		0.12±0.05
1.10	−0.16±0.04			−0.07±0.03		0.15±0.04	0.16±0.04
1.10	−0.22±0.05	−0.23±0.05	−0.15±0.04		0.15±0.04		0.11±0.05
1.20	−0.20±0.04	−0.24±0.04		−0.01±0.02		0.20±0.04	0.21±0.04
1.30	−0.14±0.03	−0.29±0.05		0.02±0.02		0.24±0.04	0.24±0.05

TABLE IV. Polarization P ($\theta_{c.m.}$) for Li^7.

E_{lab} (MeV)	P (c.m.) 23°	58°	80°	93°	111°	124°	155°
1.40	−0.21±0.04	−0.27±0.04		0.03±0.03		0.32±0.05	0.22±0.05
1.50	−0.21±0.04	−0.29±0.05		0.02±0.03		0.30±0.05	0.29±0.06
1.60	−0.18±0.04	−0.29±0.05		0.00±0.02		0.34±0.06	0.28±0.05
1.70	−0.15±0.03	−0.25±0.04		0.00±0.03		0.34±0.05	0.32±0.08
1.80	−0.23±0.05	−0.32±0.05		−0.08±0.04		0.35±0.07	0.32±0.07
1.90	−0.22±0.04	−0.34±0.05		−0.01±0.03		0.47±0.07	0.33±0.06
2.00	−0.22±0.04	−0.31±0.05		−0.03±0.03		0.38±0.06	0.30±0.06

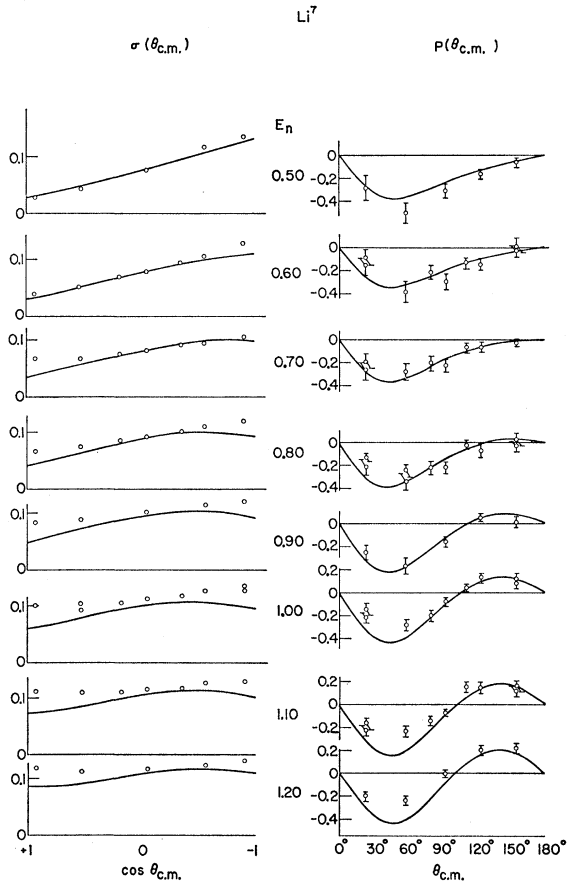

FIG. 5. Angular distributions of $\sigma(\theta)$ and $P(\theta)$ for Li^7 at incident energies of 0.5 through 1.2 MeV. The solid curves are the results of calculation (C) described in Table V. Statistical errors on $\sigma(\theta)$ are less than 2%, while the total error is probably less than 5%.

nuclides display pronounced peaks in the B_L coefficients, while Li^7 shows a strong peak in the coefficient C_1 which is some 3.5 times that for Li^6 (note the break in scale for C_1 at the Li^7 resonance in Fig. 10) and opposite in sign. Above 0.5 MeV, the coefficients B_L and C_L for both Li^6 and Li^7 are slowly varying, and both nuclides exhibit strong negative C_2 terms. (This behavior reflects the dominance of the polarization shape $-A \sin 2\theta$.) The fact that C_2 clearly dominates over C_1 in the case of Li^7 suggests that relatively simple coupling of angular-momentum quantum numbers might be adequate to explain the results. Li^6, on the other hand, shows a C_1 term comparable to that of C_2. At the higher energies, the coefficients B_1 and B_2 for both Li^6 and Li^7 are much less than B_0. This implies that the contribution from partial waves with $l>0$ is relatively small.

DISCUSSION AND INTERPRETATION

1. Li^6+n: Qualitative Considerations

The behavior of the measured differential cross sections and polarizations for neutrons scattered from Li^6 at energies less than 0.5 MeV is determined largely by the resonance at $E_n=0.25$ MeV. As mentioned above, this corresponds to a state having $J^\pi=\frac{5}{2}^-$ in Li^7 at 7.47 MeV excitation energy formed by p-wave neutrons. The polarization on this resonance is very much less than that for the similar case of Li^7+n. Since the spin of the 7.47-MeV state is $\frac{5}{2}$, it can be formed only in the orientation with channel spin $S=\frac{3}{2}$, where channel spin $\mathbf{S}=\mathbf{I}+\mathbf{i}$, I being the spin of the Li^6 ground state and $i=\frac{1}{2}$ being the neutron spin. Therefore the degree of polarization produced by the interference between the p-wave neutrons forming this state and the s-wave background neutrons would be a measure of the ratio of the s-wave background scattering in the $S=\frac{3}{2}$ channel to that in the channel with $S=\frac{1}{2}$. As Darden *et al.*[8] have shown, and as these results also show, the small values of the polarization on the resonance indicates that most of the background s-wave scattering is in the channel with $S=\frac{1}{2}$, i.e., the target and neutron have antiparallel spins. As a matter of fact, results obtained by Marshak[12]

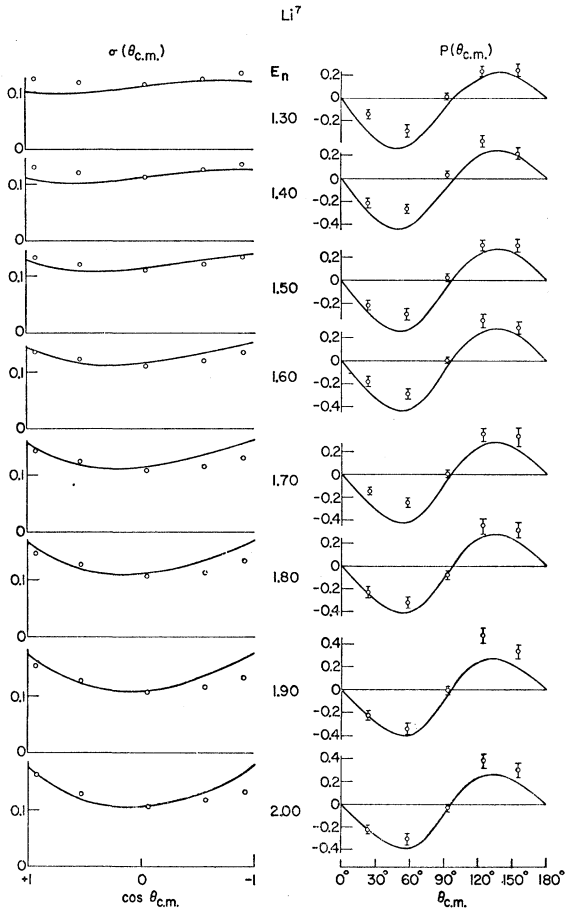

FIG. 6. Angular distributions of $\sigma(\theta)$ and $P(\theta)$ for Li^7 at incident energies of 1.3 through 2.0 MeV. The solid curves are the results of calculation (C) described in Table V. Statistical errors on $\sigma(\theta)$ are less than 2%, while the total error is probably less than 5%.

[11] L. Rosen and W. T. Leland, Phys. Rev. Letters 8, 379 (1962).
[12] H. Marshak, Bull. Am. Phys. Soc. 7, 305 (1962).

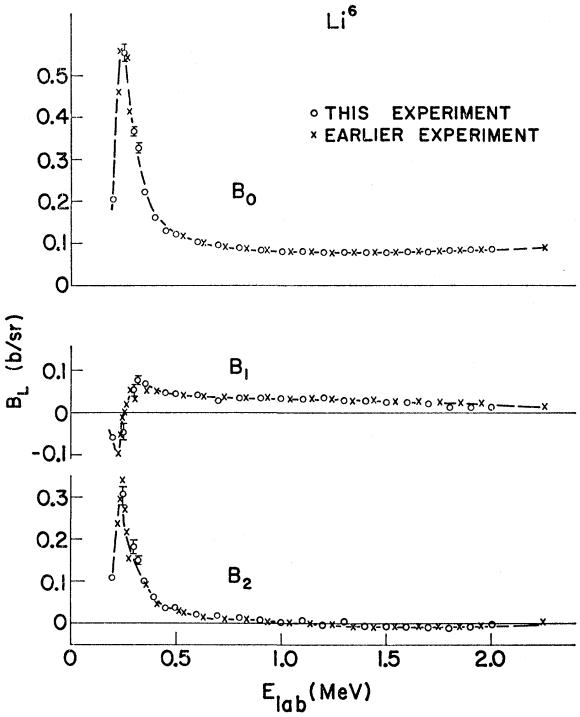

FIG. 7. Variation of B_L for Li^6 with incident neutron energy. The dashed curve is drawn through the points. The B_L for $L \geqslant 3$ are small and were neglected. Where no error bars are shown, the errors are less than the size of the points.

for the transmission of polarized neutrons through polarized Li^6 samples indicate that most of the cross section at 0.146 eV is in $S=\frac{1}{2}$. However, from fitting differential-scattering data on the resonance, Willard *et al.*[2] conclude that the *s*-wave background scattering there arises from a statistical mixture of channel spins.

At neutron energies above 0.5 MeV, both the polarization and the differential cross section become

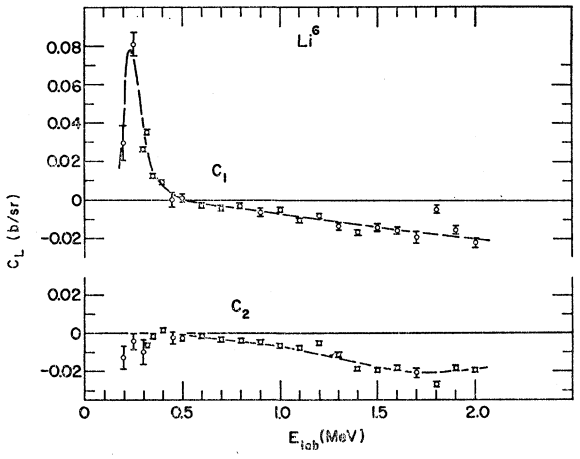

FIG. 8. Variation of C_L for Li^6 with incident neutron energy. The dashed curve is drawn through the points. The values of C_L for $L \geqslant 3$ are small and were neglected. Where no error bars are shown, the errors are less than the size of the points.

smoothly varying functions of energy, as mentioned earlier. The yield of the $Li^6(n,\alpha)H^3$ reaction is large at these energies also. In the present report, we make no further interpretation of these results, at least not in terms of possible broad levels in the compound nucleus.

2. Li^7+n: Assumed Levels in Li^8

The resonance observed at $E_n=0.25$ MeV in the total cross section for neutrons on Li^7 corresponds (as has been mentioned above) to a state in Li^8 at an excitation energy of 2.26 MeV. Several groups of investi-

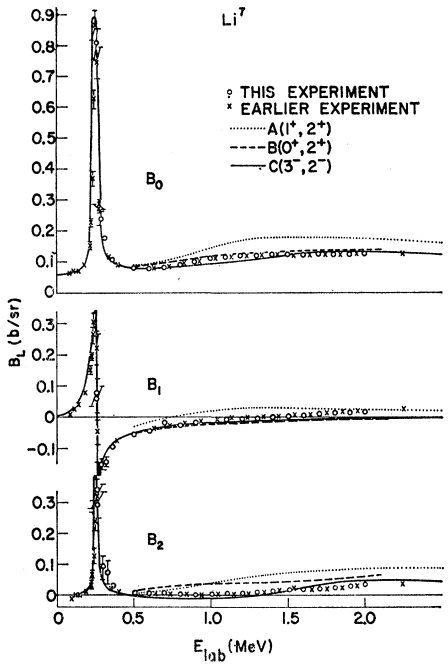

FIG. 9. Variation of B_L for Li^7 with incident neutron energy. The dotted, dashed, and solid curves are for calculations (A), (B), and (C) (Table V), respectively. The values of B_L for $L \geqslant 3$ are small and were neglected. Where no error bars are shown, the errors are less than the size of the points.

gators have pointed out that the polarizations and differential cross sections measured near this resonance are consistent with an assignment of $J^\pi=3^+$ for the total angular momentum and parity of this state, the state being excited by *p*-wave neutrons and the nonresonant background scattering being due to *s*-wave neutrons. Furthermore, the *s*-wave phase shifts were required to have a sign opposite to that produced by hard-sphere potential scattering. Since the resonance has an assignment of 3^+, it can only be formed by neutrons in the $S=2$ channel. Previous work has furthermore indicated[1,8,9] that best agreement was obtained with all the *s*-wave background scattering also confined to the $S=2$ channels. These requirements imply that a broad state having $J^\pi=2^-$ (formed by *s*-wave neutrons) may be located in Li^8 at an energy somewhat higher than the

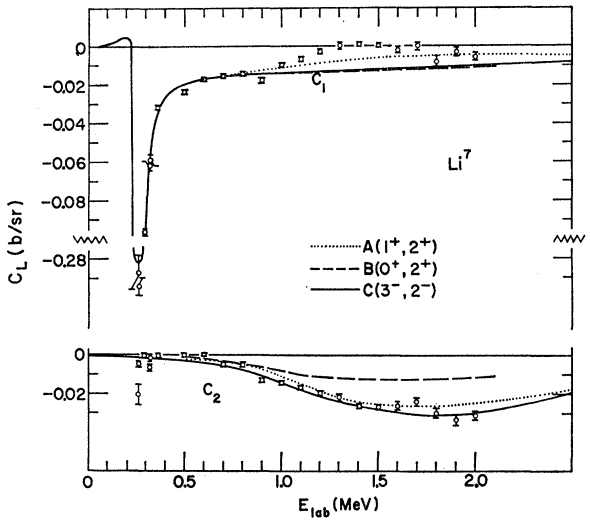

FIG. 10. Variation of C_L for Li^7 with incident neutron energy. The dotted, dashed, and solid curves are for calculations (A), (B), and (C) (Table V), respectively. The values of C_L for $L \geqslant 3$ are small and were neglected. Where no error bars are shown, the errors are less than the size of the points. Note break in scale for the resonance in the C_1 term.

resonance at 2.26 MeV. Therefore, in all of the calculations described below, we have included the level at 2.26 MeV with $J^\pi = 3^+$ and a state having $J^\pi = 2^-$ at a somewhat higher energy. In the energy region near the resonance, we have found that only these two levels were necessary to fit the measured $\sigma(\theta)$ and $P(\theta)$.

In the energy region above $E_n \approx 0.5$ MeV, where no sharp resonance dominates the interaction, the treatment of the problem in terms of levels becomes much less useful. However, it is often possible to obtain at least a qualitative description of the interaction by considering the addition of one or two postulated levels. This procedure was adopted for exploratory purposes, since little is known of the level structure of Li^8 in this region. These postulated states are assumed to be broad and to contribute the slowly varying phase shifts that are needed to bring about the best agreement with the measured differential cross section and polarization, both of which become almost constant above 1 MeV.

The differential cross sections and polarizations were calculated by use of the formalism of Blatt and Biedenharn[13] and Simon and Welton.[14] A general description of the procedure is presented in Ref. 10. For the present work (as in Ref. 10), a single-level expression for the scattering-matrix elements was considered adequate. However, the possibility of channel-spin flip in the exit channel was retained by using scattering-matrix elements for an arbitrary number of channels. The form of the matrix elements is given by Eq. (5) in Ref. 10. In all of the present work the positive sign for the square root $(\Gamma_c \Gamma_{c'})^{1/2}$ [in Eq. (5)] is used. All of the calculations were programmed in FORTRAN language and performed on the CDC-3600.[15]

The best-fit parameters for the 3^+ state at 2.26 MeV and a 2^- state (which were retained in all fitting attempts) are shown in Table V as the first two lines for each of the three sets of calculations listed. In Table V, γ_{SlJ}^2 is the partial reduced width and E_λ is the

TABLE V. Values of level parameters assumed for calculations for Li^7+n. With the exception of the 3^+ state, these values should be regarded only as attempts to fit the data and not as assignments.

E_r (MeV, lab)	J^π	l	S	γ_{SlJ}^2 $S=1$	$S=2$	E_λ (MeV, c.m.)
			(A)			
0.25	3^+	1	2	0	0.307	−0.043
3.4	2^-	0	2	0	2.28	3.0
1.5	1^+	1	1, 2	1.5	1.5	−0.2
3.0	2^+	1	1	3.0	0	1.55
			(B)			
0.25	3^+	1	2	0	0.307	−0.043
3.4	2^-	0	2	0	2.28	3.0
1.0	0^+	1	1	3.0	0	−0.7
3.0	2^+	1	1	3.0	0	1.55
			(C)			
0.25	3^+	1	2	0	0.307	−0.043
3.4	2^-	0	2	0	2.28	3.0
···	3^-	2	1, 2	Empirical set of phase shifts[a]		

[a] See Fig. 12.

characteristic energy. The determination of level parameters for such a 2^- state is not completely definite. Our choice in the calculations was determined by the conditions that the phase shift produced by the state should (i) give the proper nonresonant background below $E_n \approx 0.5$ MeV, (ii) produce (with the aid of the 3^+ state) the observed energy dependence of $\sigma(\theta)$ and $P(\theta)$ near the resonance, and (iii) give slowly varying values of $\sigma(\theta)$, $P(\theta)$, and total cross section above the resonance. A radius of 4.0 F was used in all calculations of the penetration and shift factors (see Ref. 10). It is clear that reasonably good agreement with the measured cross sections and polarizations is obtained in the vicinity of the 0.25-MeV resonance (Figs. 4, 9, and 10). This was true for all three combinations of broad states and phase shifts introduced to fit the higher-energy data. The interference between the 3^+ and 2^- states and the other levels introduced was always taken into account.

As mentioned previously, in the neutron energy region above 0.5 MeV the polarization is dominated by an angular dependence of the form $-A \sin 2\theta$. This leads

[13] J. M. Blatt and L. C. Biedenharn, Rev. Mod. Phys. **24**, 258 (1952).

[14] A. Simon and T. A. Welton, Phys. Rev. **90**, 1036 (1953).

[15] As a check on the computer code, the differential cross sections and polarizations for neutrons scattered from a zero-spin nucleus were calculated and compared with similar calculations performed with *two* different codes. One was the ABACUS-2 code and the other a program described earlier by the authors [R. O. Lane, A. J. Elwyn, and A. Langsdorf, Jr., Phys. Rev. **126**, 1105 (1962)]. All the results agreed with each other.

to a dominant coefficient C_2 in the expansion of the differential polarization $\sigma_p(\theta)$. Such an even-L term arises from the interference of neutron partial waves of the same parity. Thus, one might expect such a term to arise at these energies because of interference either between states formed by p-wave neutrons or between states formed by s- and d-wave neutrons.

On the basis of shell-model considerations, the presence of normal-parity (positive) states of character 0^+, 1^+, 2^+, and 3^+ would be most likely predicted. Such states would be formed by p-wave neutrons. Thus, in the first calculations, we tried pairs of broad states with the spins and parities listed above.

Tables V(A) and (B) list the spins, parities, and parameters of two combinations of positive-parity states (as well as the properties of the 3^+ and 2^- levels discussed above). The results of calculations based on these values are shown as the dotted and dashed curves in Figs. 9 and 10. These represent the best fits obtained but do not give good fits to both coefficients B_L and C_L simultaneously. Other pairs of positive-parity states such as 1^+ and 3^+, and 2^+ and 3^+, as well as the addition of a 1^+ state at $E_n=1.35$ MeV as described by Freeman *et al.*,[4] disagreed much more with the data than those shown.

In Fig. 11 we have plotted both the differential cross section and polarization as a function of angle at $E_n=1.7$ MeV and compared the measurements with the calculations given in Tables V(A) and (B). The curves at this energy are fairly typical of the general trend at energies above 1 MeV. For neither case do both the calculated $P(\theta)$ and $\sigma(\theta)$ agree well with the data.

Negative-parity states in Li^8 would most probably be formed at these neutron energies by partial waves $l=0$ and 2. We have therefore considered combinations of states leading to d-s interference in the neutron partial waves.

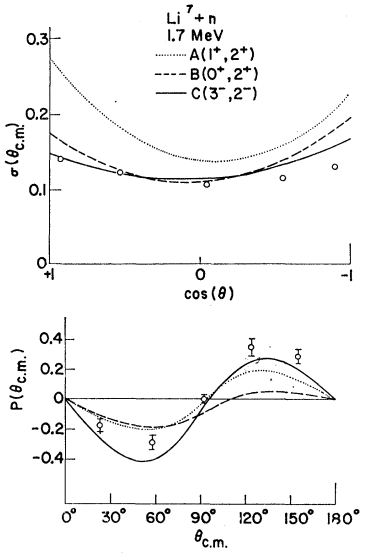

FIG. 11. Comparison of experimental $\sigma(\theta)$ and $P(\theta)$ with those of calculations (A), (B), and (C) (Table V).

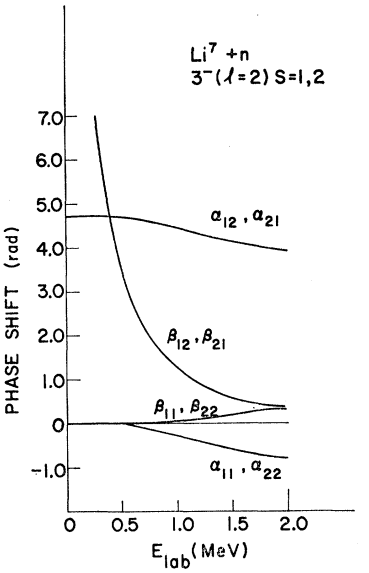

FIG. 12. Variation of phase shifts of calculation (C) (Table V) with energy.

To keep the number of states involved to a minimum, the 2^- level (formed by s-wave neutrons) necessary to fit the data in the vicinity of the resonance was retained as one member of the pair, while the d-wave contribution was taken to arise from a state having spins and parities of either 0^-, 1^-, 3^-, or 4^-. Only for the case of a state with $J^\pi=3^-$ did interference with the 2^- level give reasonable agreement with the measurements.[16] However, such a level had to be so broad that the concept of a state seemed to have little meaning in the usual sense. The $J^\pi=3^-$ contribution was therefore replaced by a set of slowly varying phase shifts; and the scattering matrix elements [Eq. (5) of Ref. 10] were replaced by a two-channel scattering matrix, defined as

$$U_{c'c}=\exp[i(\alpha_{c'c}+i\beta_{c'c})],$$

where channels c' and c refer to the two channel spins $S=1$ and 2. The phase shifts $\alpha_{c'c}$ and $\beta_{c'c}$ that gave the best fit to the measurements are shown in Fig. 12.

Table V(C) gives the spins and parities of the set of levels for the case of negative-parity states. The results of the calculations utilizing the properties of the 3^+ and 2^- states and the phase shifts of Fig. 12 are shown as the solid curves in Figs. 4–6 and 9–11. These results are in fair agreement with the data except for two systematic differences. At the higher energies, the calculated polarization lies systematically below the data. Furthermore, from 0.8 to 1.3 MeV, the calculated and experimental curves of differential cross sections have opposite curvature. The inclusion of a state having $J^\pi=1^+$ or 1^- as described by Freeman *et al.* did not improve

[16] It should be mentioned that only the process of channel-spin flip from $S=2$ to $S=1$ in the $J^\pi=3^-$ state leads to polarization. The process for no spin-flip leads to zero polarization because the X coefficient [see Eq. (4) of Ref. 10] accidentally vanishes for the quantum numbers involved in this process.

the fits to the data in this energy region. Another process considered with the negative-parity states in Table V(C) was the one in which a state with $J^\pi=1^-$ or 2^- might contribute by the two-channel process of formation and decay with a net change $\Delta l=2$ in the orbital angular momentum (for example, formation of the state by $l=0$ neutrons and decay by $l=2$ neutrons). However, all of the several combinations of parameters tried produced results which were in poorer agreement with the data than the calculations discussed above.

In summary, for $n+\mathrm{Li}^7$, the data near 0.25 MeV can be fitted rather well for the assignment $J^\pi=3^+$ with the resonance formed by p-wave neutrons in the channel $S=2$ together with an s-wave background in channel $S=2$ only, and produced by a 2^- state at higher energy. For energies of 0.5–2.0 MeV, the best fit to the data was obtained with the addition of phase shifts of the character $J^\pi=3^-(l=2)$, $S=1$, 2 where channel-spin flip is allowed. The assumptions tried here represent only a few of the simpler and more obvious ones. For a nucleus such as Li^7 with spin $I=\frac{3}{2}$, the permutation of possible quantum numbers and choices of certain phase factors together with possible variations of level widths, positions, channel-spin mixtures, radius of interaction, etc., reaches a very large number. One of the most difficult problems at the higher energies is the fact that $\sigma(\theta)$ and $P(\theta)$ vary so slowly with energy that there is no clear indication that any one state or partial wave dominates the situation as it does on the resonance at 0.25 MeV. Such a slow variation may indeed be a superposition of the effects of several distant states. If such is the case, the problem of searching for combinations to fit the data is a large undertaking. Such an approach would probably be meaningful only if detailed nuclear model calculations were carried out to predict the character of highly excited nuclear states.

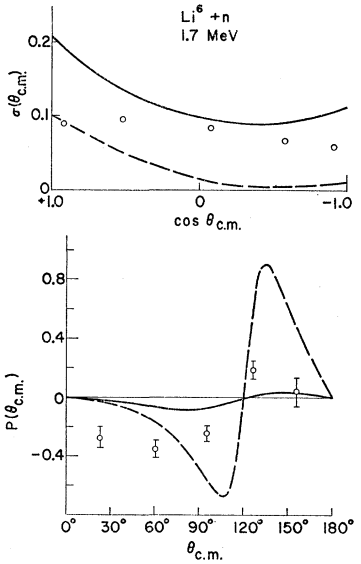

FIG. 13. The measured differential cross sections and polarizations for neutrons scattered from Li^6 at 1.7 MeV compared with an optical-model calculation. The dashed curve is the calculation for shape elastic scattering only; the solid curve includes compound elastic scattering as calculated by the theory of Hauser and Feshbach. The optical model employed is a local model equivalent to the nonlocal potential of Ref. 17 plus an added spin-orbit potential. In the notation of Ref. 18, the parameters in the present case are $V_L=47.54$ MeV, $W_L=9.72$ MeV, $a_S=0.68$ F, $a_D=0.47$ F, $r_0=1.34$ F, $V_S=10$ MeV, and $W_S=0$.

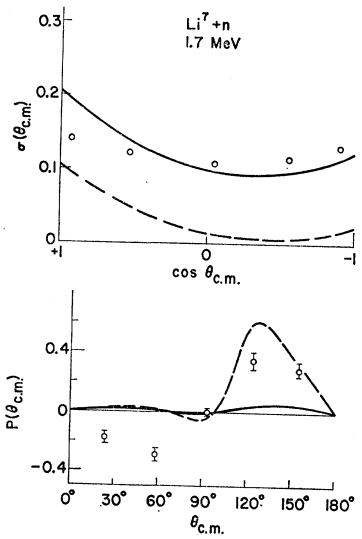

FIG. 14. The measured differential cross sections and polarizations for neutrons scattered from Li^7 at 1.7 MeV compared with an optical-model calculation. The dashed curve is the calculation for shape-elastic scattering only; the solid curve includes compound elastic scattering as calculated by the theory of Hauser and Feshbach. The optical potential employed is a local potential equivalent to the nonlocal potential of Ref. 17, plus an added spin-orbit potential. In the notation of Ref. 18, the parameters in the present case are $V_L=47.42$ MeV, $W_L=9.78$ MeV, $a_S=0.68$ F, $a_D=0.47$ F, $r_0=1.34$ F, $V_S=10$ MeV, and $W_S=0$.

3. Li^6+n and Li^7+n: Optical-Model Considerations

Batchelor and Towle[5] have suggested that the differential cross sections in the scattering of neutrons from both Li^6 and Li^7 at energies from 1.5 to 7.5 MeV can be understood reasonably well on the basis of an optical-model interaction. The model that they employed was the nonlocal optical potential of Perey and Buck[17]; the calculations were performed by use of an equivalent local potential which had been obtained from Eq. (35) of Ref. 17. No spin-orbit potential was included.

In the present work, we have calculated the polarization and differential cross sections at energies from 0.5 to 2.2 MeV by use of the potential of Perey and Buck. As in the report of Batchelor and Towle, the work was done with an equivalent potential, the parameters being obtained by use of Eq. (35) of Ref. 17, as described in more detail be Elwyn *et al.*[18] The calculations were performed by use of the ABACUS-2 computer program[19] and the IBM-704 computer. In the present calculations we employed a real spin-orbit potential of the Thomas

[17] F. Perey and B. Buck, Nucl. Phys. **32**, 353 (1962).

[18] A. J. Elwyn, R. O. Lane, A. Langsdorf, Jr., and J. E. Monahan, Phys. Rev. **133**, B80 (1964).

[19] E. H. Auerbach, Brookhaven National Laboratory Report BNL-6562 (unpublished).

form. Compound elastic scattering was accounted for by use of the theory of Hauser and Feshbach.[20]

The results of the calculations show fair agreement with the measured total and differential cross sections, especially for the case of Li^7. The fits to the polarization measurements, on the other hand, were somewhat worse. Typical examples of the kind of agreement that was obtained are shown in Figs. 13 and 14. The solid curves on these figures show the calculations including compound elastic scattering. The dashed curves show only the shape-elastic predictions.

We have made preliminary attempts to improve the fits by studying the effect of varying some of the optical-model parameters. A variation of the parameters of the spin-orbit potential did not lead to improved agreement with the data when the values of the other parameters were kept fixed at those strengths predicted by the nonlocal model. Further variation of parameters from those predicted by the nonlocal model have led so far to only qualitative conclusions. For example, it appears that better agreement with the data might be obtained with somewhat smaller values for the strength of the imaginary central potential. Recently, Perey and Saxon[21] have pointed out that a "better" local approximation to the nonlocal potential defined in Ref. 17 can be obtained. Perey[22] has pointed out that one of the results coming from their study is that the values of the diffuseness of the real well differ from those values predicted by Eq. (35) in Ref. 17. Accordingly, we studied the effect of varying this parameter over a wide range. No substantial improvement in the agreement with the data was found. We hope to continue further work toward obtaining a more realistic optical potential for these nuclei in the energy range below 2 MeV.

[20] W. Hauser and H. Feshbach, Phys. Rev. 87, 366 (1952).

ACKNOWLEDGMENTS

The authors wish to thank Dr. J. E. Monahan for useful discussions, D. Jordan for use of his subroutines for angular-momentum coupling coefficients, W. Ray, R. Amrein, and the crew of the Argonne 4.5-MeV Van de Graaff accelerator for their assistance in the experiment, and D. Mueller, R. Obenchain, B. Blumenstein, and C. Walker for aid in data reduction.

[21] F. G. Perey and D. S. Saxon (to be published).
[22] F. G. Perey (private communication).

PHYSICAL REVIEW VOLUME 136, NUMBER 6B 21 DECEMBER 1964

Thresholds for (p,n) Reactions on 26 Intermediate-Weight Nuclei*

C. H. JOHNSON, C. C. TRAIL,† AND A. GALONSKY‡
Oak Ridge National Laboratory, Oak Ridge, Tennessee
(Received 12 August 1964)

Protons with energies below 5 MeV, produced by either a 3-MV or a 5.5-MV Van de Graaff accelerator, were used to find (p,n) thresholds and threshold limits for 26 nuclei with $37 \leq A \leq 112$. Data are presented from several independent measurements which were made over a period of about five years; the present values supersede those presented in earlier abstracts by Trail and Johnson and by Johnson and Galonsky. Energy calibrations are based on one or more of the following absolute standards: $^7Li(p,n)$, 1880.7±0.4 keV; $^{11}B(p,n)$ 3016.4±1.5; $^{19}F(p,n)$, 4234.4±1.0 keV; and $^{19}F(p,\alpha\gamma)$, 872.5±0.4, 934.1±0.9, 1346.6±1.1, and 1373.5±0.6 keV. Neutrons were detected in each experiment by several BF_3 counters in 4π geometry. The yields near threshold have been interpreted in terms of the Hauser-Feshbach statistical theory of the compound nucleus, and in most cases there is good agreement with the predictions for the ground-state transitions. The targets and the corresponding negative Q values in keV for these ground-state transitions are as follows: ^{37}Cl, 1596.9±2.5; ^{41}K, 1209.7±1.5; ^{49}Ti, 1383.6±1.0; ^{51}V, 1533.7±1.8; ^{53}Cr, 1380.4±1.6; ^{55}Mn, 1014.4±0.8; ^{57}Fe, 1619±2; ^{59}Co, 1855.3±1.6; ^{61}Ni, 3024±4; ^{65}Cu, 2135.8±1.7; ^{67}Zn, 1783.3±1.4; ^{68}Zn, 3707±5; ^{69}Ga, 3006±4; ^{70}Zn, 1439±3; ^{71}Ga, 1018±2; ^{74}Ge, 3348±5; ^{75}As, 1647.3±1.1; ^{80}Se, 2653±3; ^{106}Pd, 3754±13; ^{108}Pd, 2670±100; and ^{112}Cd, 3400±20. In addition, three thresholds were observed for which the comparison of the observed yields with the predictions indicates that the reactions proceed to the excited states in the residual nuclei. The three targets and the corresponding negative Q values in keV are as follows: ^{73}Ge, 1189±15; ^{89}Y, 4207±6; ^{93}Nb, 2720±100. The fact that the $^{93}Nb(p,n)^{93}Mo$ threshold to the 1.48-MeV state was observed indicates that lower states in ^{93}Mo have $J \leqslant \frac{5}{2}$. For three other targets the yield curves showed some indication of a threshold; however, comparisons with the theory in these cases indicate that only the following upper limits can be set to $-Q$ in keV: $^{48}Ca(p,n)^{48}Sc$, <640; $^{82}Se(p,n)^{82}Br$, <920; $^{93}Nb(p,n)^{93}Mo$, <1290. A comparison with the theory indicates that the observed yield above 650 keV for ^{48}Ca must be due to a transition to an excited state rather than the ground state of ^{48}Sc.

I. INTRODUCTION

THE mass difference between two isobars can often be found with ease and precision by observing the (p,n) reaction threshold for a ground-state transition. If the residual nucleus is unstable against positron emission, the negative of the Q value must be greater than 1804 keV; in this case the threshold energy

* Research sponsored by the U. S. Atomic Energy Commission under contract with Union Carbide Corporation.

† Present address: Brooklyn College, Brooklyn, New York.
‡ Present address: Michigan State University, East Lansing, Michigan.